Proceedings World Geothermal Congress 2023
Beijing, China, April 17 – 21, 2023

Characterization of Ground Thermal Conditions for Shallow Geothermal Exploitation in the Central North China Plain (NCP) Area

Wan L. Wang, Gui L. Wang, Feng Liu and Chun L. Liu

268 Northe Zhonghua Street, Shijiazhuang, Hebei Province, China

wangwanli@mail.cgs.gov.cn; wangguiling@mail.cgs.gov.cn; liufeng@mail.cgs.gov.cn; liuchunlei@mail.cgs.gov.cn

Keywords: ground source heat pump systems (GSHPs); thermal conductivity; hydrogeological settings; thermal response test (TRT); constant heating-temperature method (CHTM); the center North China Plain (NCP)

ABSTRACT

The North China Plain (NCP) is one of the rapid developing regions in China which has great potential for ground source heat pump (GSHP) system applications. Currently, only limited data of ground thermal properties, which is the prerequisite for GSHP systems design, can be obtained. In this paper, the ground thermal conditions including ground temperature and thermal conductivity are characterized in three representative hydrogeological regions in the NCP area: the piedmont alluvial plain, the central alluvial plain, and the coastal plain. Results show that the geothermal gradient below 40 m in depth in this area ranges from 0.018 °C/m to 0.029 °C/m. Thermal conductivity measured in laboratory ranges between 1.52 and 1.79 W/(m·K), with a standard deviation varying between 0.16 and 0.89. Thermal conductivity in the piedmont plain exhibits a larger variability than that of the central and coastal plain due to the significant heterogeneity of lithology.

1. INTRODUCTION

Due to the energy-saving, high efficiency, and environmental friendliness (Zeng et al.,2003, Blum et al., 2010) advantages, ground source heat pump systems (GSHPs) have developed rapidly in recent years . Up to the year 2019, the installed capacity of GHSPs accounted for 71.6% of the global total installed capacity of geothermal energy utilization (Lund et al., 2021). The North China Plain (NCP), which is a major economic center of China, is one of the regions with abundant geothermal energy. Based on investigations of the geothermal resources in the shallow ground of the major cities of the NCP, it has been shown that shallow geothermal energy can satisfy the space heating and cooling for an area of 1600–3500 km^2 (Wang et al., 2017). Up to the year 2015, a total building area of 85 km2 for both heating and cooling has been installed in the main cities of the NCP. However, for rural areas of the NCP, inefficient bulk coal has been commonly utilized for space heating as a centralized heating system was not available, causing air pollution in the winter (Tao et al., 2018, Wang et al., 2021). Therefore, clean energy such as geothermal energy is preferentially recommended for these areas. Although the hydrogeologic conditions of the NCP are well studied, the understanding of the main controls affecting the efficiency of GSHP systems in the NCP is limited.

In this study, the ground thermal properties of the central NCP are determined in three representative hydrogeological regions: the piedmont alluvial plain, the central alluvial plain, and the coastal plain. Temperature sensors were installed at different depths to obtain ground temperature profiles in the typical boreholes of nine cities located in these regions, and laboratory measurements were performed to estimate the thermal conductivity.

2. MATERIALS AND METHODS

2.1 Geological settings

The NCP is the largest plain in east Asia, occupying an area of 140,000 km^2 (Cao et al., 2016). The area has a continental, semi-arid climate with a mean annual temperature of 12-13°C and the mean annual precipitation ranges from 500 to 600 mm (Zongyu et al., 2003). The NCP is bounded by the Yanshan Mountain to the north, the Taihang Mountain to the west and the Bohai Bay to the east, and elevation gradually decreases from 100 m to 2–3 m above sea level (Foster et al., 2004). The whole region can be divided into piedmont alluvial plain (I), central alluvial plain (II) and coastal plain (III) from the west to the east (Shu et al., 2012, Wang et al., 2014, Li et al., 2011) (Fig. 1). The Cross section A-A' (shown in Fig. 1), which crosses through the three different geological units, has been widely used in studies on groundwater recharge, groundwater chemical evolution, and groundwater flow systems of the NCP (Chen et al., 1999, Zhang and Fei, 2009, Xing et al., 2013). Based on abundant borehole data, Fig. 2 summarizes the distribution of Quaternary aquifer units and the pattern groundwater flow along the cross section

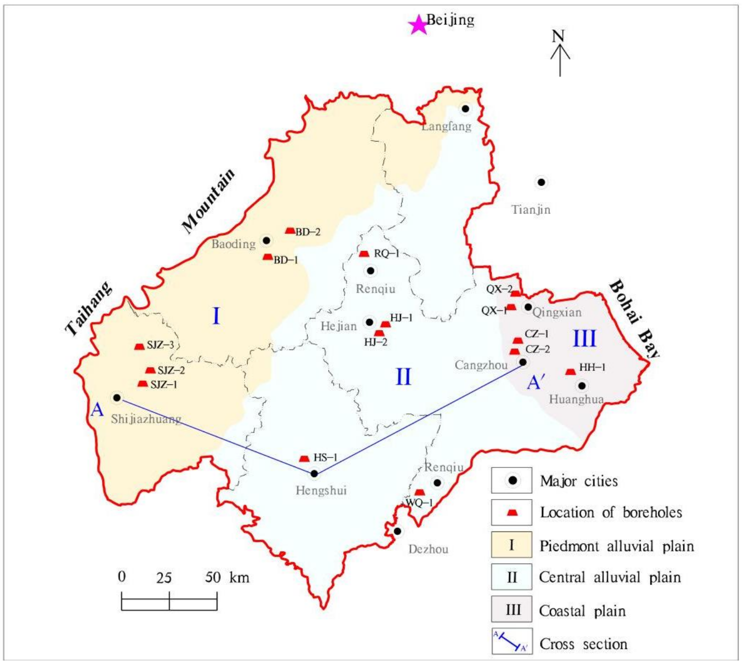

Figure 1: Map of the central North China Plain.

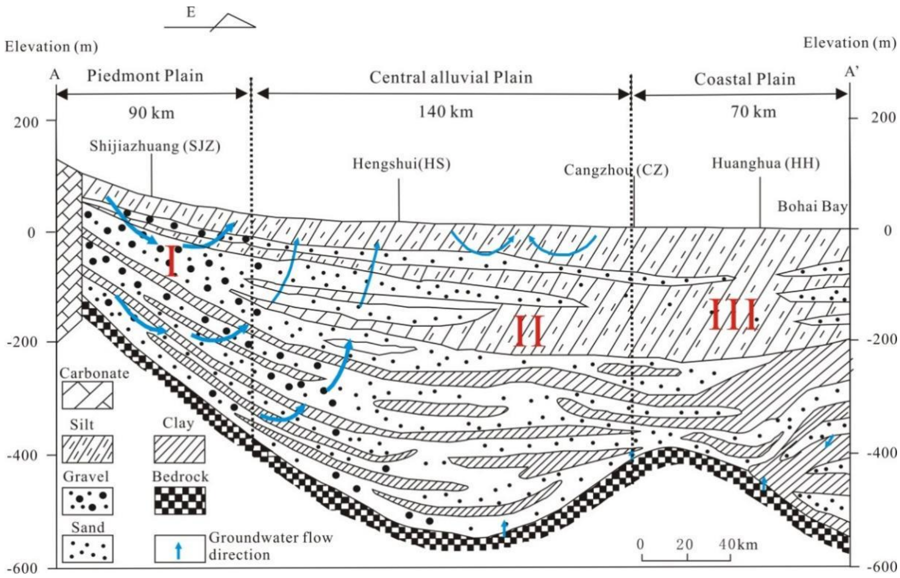

Figure 2: Conceptual cross-section along the A-A' line (modified after (Cao et al., 2016, Li et al., 2011, Xing et al., 2013)).

General features of the representative regions are shown in Table 1. For the piedmont alluvial plain, the Quaternary sediments within 200 m are dominated by sand, gravel, and clay with great inhomogeneity (Xing et al., 2013). The Quaternary aquifer is unconfined and is recharged by infiltration of atmospheric precipitation and lateral flow from mountains. With a relatively high hydraulic conductivity and high specific yield, groundwater flow velocity in this region ranges between 0.013 and 0.26 m/d (Xing et al., 2013) and the water table depth ranges between 20 and 45 m (Lu et al., 2011). The cities of BD and SJZ are representative cities of this region.

Table 1: General features of the representative regions.

Hydrogeological Setting	Representative Region	Water Table Depth (m)	Groundwater Flow Velocity (m/d)	Lithology (<150 m)
Piedmont Plain (I)	BD and SJZ	20–45	0.013–0.26	Gravel, sand, silt, and clay
Central Plain (II)	HS, RQ, HJ, and WQ	3–5	0.002–0.10	Clay, silty clay, and silt
Coastal plain (III)	CZ, QX, and HH	1–5	0.002–0.10	Silt and silty clay

2.2 Test Sits and Borehole Setting

In the current study, 15 boreholes were drilled within the three representative regions. Among them, 5 boreholes are in BD and SJZ cities, representing the piedmont alluvial plain (I), 5 boreholes are in RQ, HJ, WQ, and HS cities, representing the central alluvial plain (II), and 5 boreholes are in HH, QX and CZ cities, representing the coastal plain (III) (Figure 1). Because the boreholes are used for shallow geothermal energy, the depth of all boreholes is within 150 m.

Before conducting the relevant tests, hydrogeological investigations were carried out in the study area to obtain the groundwater level of the wells and then the water-level contour map of the area was plotted. Following this, the hydraulic gradient was obtained and, combined with the permeability of the aquifer, the groundwater flow velocity was estimated at each borehole location. Detailed information on the 15 boreholes is shown in Table 2.

Table 2: Borehole and equipment installation details.

Hydrogeological Setting	Borehole	Depth (m)	Water Table Depth (m)	Groundwater Flow Velocity (m/d)	Temperature Sensor
Piedmont plain (I)	BD-1	100	25	0.085	√
	BD-2	100	15	0.04	√
	SJZ-1	100	45	0.138	
	SJZ-2	120	42	0.1162	√
	SJZ-3	120	38	0.2125	√
Central plain (II)	RQ-1	120	5	0.005	√
	HJ-1	150	5	<0.005	
	HJ-2	120	5	<0.005	√
	WQ-1	120	5	0.005	√
	HS-1	100	5	0.005	
Coastal plain (III)	CZ-1	100	4	0.005	
	CZ-2	120	4	<0.005	
	HH-1	150	3	<0.005	√
	QX-1	120	3	<0.005	
	QX-2	120	3	<0.005	√

Sediments of boreholes in BD and SJZ have coarse particle sizes, such as gravel, coarse sand, and medium sand, while sediments of boreholes in other cities have a relatively finer particle size of silt and silty clay. Soil samples were collected every 5 m at each borehole and then covered by a plastic membrane to prevent moisture loss before sending to the laboratory. Texture, bulk density, water content, and thermo-physical properties were analyzed by the Hebei University of Technology.

The thermal conductivity of soil samples was measured by a KD2 device (Decagon Devices, Pullman, WA, USA) in line with ASTM Standard D5334-00. This device follows the principle of an infinite line heat source, and the sample should have a certain thickness to avoid boundary effects during the test. When the temperature of the heat source ranges between 5 and 40 ℃, the device has 5% accuracy (Kharazmi et al., 2015). The samples were tested as soon as possible after being sent to the laboratory to maintain the original humidity and were tested under natural pressure.

After drilling was completed, a DN32 double-U-shaped BHE was installed into the borehole. In order to reduce the test measurement error, the length of the above-ground section of the BHE was retained for about 1 m and insulated to minimize heat loss. For long-term monitoring of the ground temperature, calibrated PT1000-type temperature sensors with 0.1 °C accuracies were installed at different depths of the outside of the U-pipes and buried in the borehole. In addition, a data acquisition recorder was used to collect temperature distributions at 10 min intervals. For financial considerations, only 2–4 boreholes were selected in each hydrogeological setting. The temperature sensors were equipped at 5 m intervals within 50 m of depth, and at 10 m intervals when deeper than 50 m.

3. RESULTS AND DISCUSSIONS

3.1 Ground Temperature

The borehole temperatures of nine boreholes were first collected. Figure 3 presents the ground temperature profiles of these boreholes.

The temperature profiles of the nine boreholes show a similar tendency and three temperature sections can be distinguished: (1) a shallow section (including the surface part), where the ground temperature is mostly affected by climatic conditions, including air temperature, solar radiation, etc., (2) a constant-temperature section, where the ground temperature is relatively stable and is similar to the average surface ground temperature (Badache et al., 2016), and (3) a deep section, where the temperature increases with depth and the slope of the curve called geothermal gradient. This phenomenon is identical to other previous research areas (Popiel et al., 2003, van Manen and Wallin, 2012).

In the four typical boreholes at the piedmont plain, the ground temperature within the 15 m depth is highly influenced by seasonal atmospheric conditions and the influence reduces as the depth increases (Figure 3a). The middle section between 15 m and 40 m has a relatively constant ground temperature which ranges from 13.59 °C in SJZ-2 and 14.27 °C in BD-2. The temperature gradient in North China normally ranges from 0.02–0.03 °C/m (Wang et al., 2021). For boreholes BD-1 and SJZ-3, the deep section below 40 m in depth has normal temperature gradients of 2.45 and 2.87, while for boreholes SJZ-2 and BD-2, the temperature gradients are only 0.018 °C/m and 0.019 °C/m, respectively, which are lower than the normal range. Table 4 lists the main lithology of borehole SJZ-2. The gravel layer (fine sand, coarse sand, and gravel) covers 58% of the layer thickness. Especially for depths from 47 m to 93 m, the ground is dominated by coarse sand and gravel which has a relatively strong groundwater flow and high hydraulic conductivity. The ground temperature rises slowly compared to other boreholes due to the strong cooling effect of groundwater flow on the surrounding ground (Wang et al., 2009). For the deep section, the ground temperature is dominated by convection instead of conduction which leads to a lower gradient (Radioti, et al., 2017, Wang et al., 2009, Xiong et al., 2015). The same phenomenon occurred in borehole BD-2.

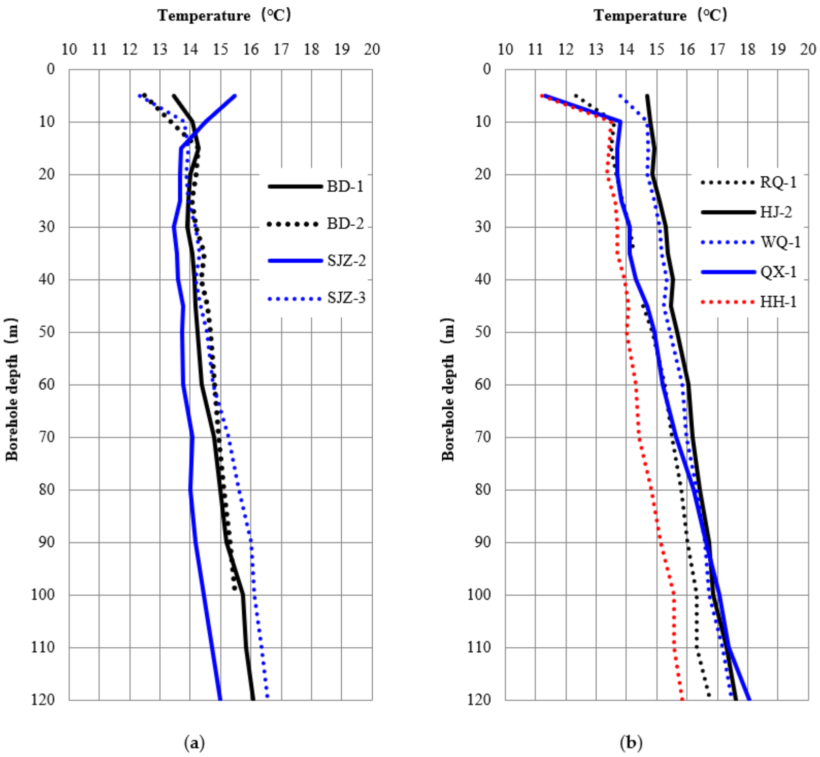

Figure 3: Undisturbed ground temperature profile: (a) the piedmont pain; (b) the central and coastal plain.

RQ-1, HJ-2, and WQ-1 are three boreholes located in RQ, HJ, and WQ in the central alluvial plain (Figure 3b). The ground temperature within the 10 m depth is influenced by the external environment. Between 10 m and 35 m in depth, the ground temperature keeps almost constant at 13.83 °C in RQ-1, 15.05 in HJ-2, and 14.87 °C in WQ-1. The temperature rises with an increase in depth, and the geothermal gradient is 0.026–0.029 °C/m, which is within the regular range of 0.02–0.03 °C/m in the NCP. Compared with borehole temperature profiles in the piedmont region, the central plain shows little effect from groundwater flow, which agrees with the finding of (Wang et al., 2009) that there is low horizontal groundwater velocity under the central and coastal plains.

For boreholes QX-1 and HH-1 located in the coastal plain, the shallow temperature layer presents seasonal variations up to a depth of 10 m (Figure 3b), which is similar to the temperature tendency of boreholes in the central alluvial plain. Between 10 m and 35 m in depth, the ground temperature keeps almost constant at 13.88 °C and 13.56 °C. Under this depth, the temperature rises with depth and the geothermal gradient is 0.025 °C/m.

3.2. Thermos-Physical Properties of the Geological Materials

To obtain the ground thermal properties, soil samples were collected every 5 m along a borehole, which leads to a total of 352 samples from the 15 boreholes. These samples include silty clay, silt, fine sand, silty-fine sand, medium-coarse sand, and coarse sand. The thermal conductivity of soil samples was measured by a KD2 device (Decagon Devices, USA) with a transient line heat source. Figure 4 shows the thermal conductivity of the soil samples at different depths of the 15 boreholes.

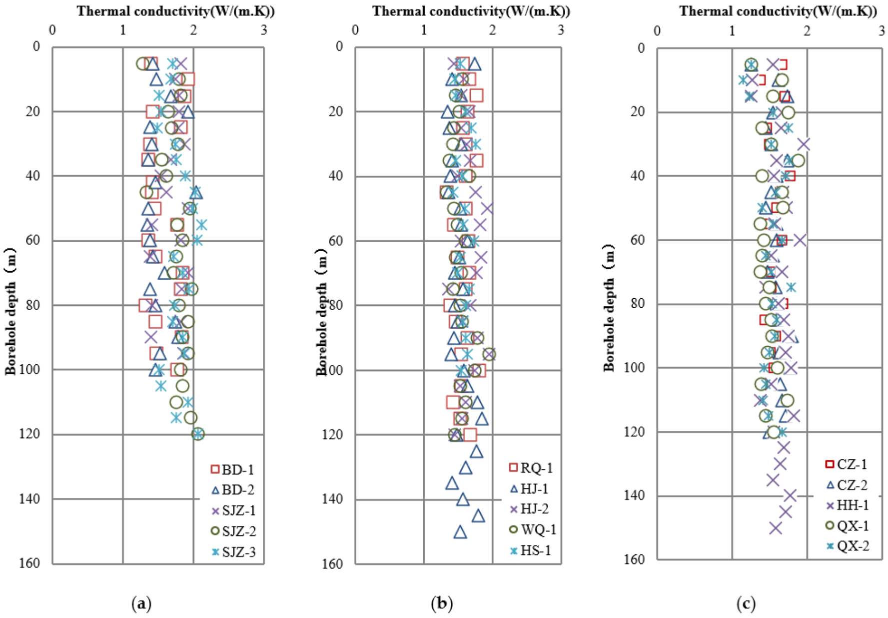

Figure 4: Vertical distribution of the thermal conductivity of locations in different regions: (a) the piedmont plain; (b) the central plain; and (c) the coastal plain.

The minimum, maximum, and the standard deviation of the thermal conductivity of the 15 boreholes were then calculated and listed in Table 4. The thermal conductivity of boreholes in the piedmont plain ranges from 1.28 to 2.11 W/(m·K), with a standard deviation varying between 0.62 and 0.89. For the central alluvial plain, this value ranges from 1.33 to 1.95 W/(m·K), with a standard deviation varying between 0.16 and 0.56. For the coastal plain, the thermal conductivity ranges from 1.14 to 1.95 W/(m·K), with a standard deviation varying between 0.21 and 0.69. Thermal conductivity in the piedmont plain exhibits a larger variability than that of the central and coastal plain due to the significant heterogeneity of the lithology. As mentioned in Section 2.1, the Quaternary sediments within 200 m depth in the piedmont plain are dominated by sand, gravel, and clay with great inhomogeneity, however, the Quaternary sediments within 200 m are dominated by fine-grained deposits of silt and clay materials.

The laboratory mean thermal conductivity of each borehole was obtained by the arithmetic mean method and listed in Table 5. It was found that the five boreholes in the piedmont plain have an average thermal conductivity varying between 1.53 and 1.79 W/(m·K). The six boreholes in the central alluvial plain have an average thermal conductivity varying between 1.54 and 1.64 W/(m·K), and the four boreholes in the coastal plain have an average thermal conductivity varying between 1.52 and 1.62 W/(m·K). The thermal conductivity measured by soil samples differs slightly among the three regions.

Table 4: Deviation of laboratory measurements of thermal conductivity in boreholes.

Hydrogeological Setting	Borehole	Min (W/(m·K))	Max (W/(m·K))	Standard Deviation	Mean (W/(m·K))
Piedmont plain (I)	BD-1	1.32	1.92	0.75	1.53
	BD-2	1.34	2.03	0.89	1.57
	SJZ-1	1.39	1.92	0.62	1.70
	SJZ-2	1.28	1.97	0.79	1.77
	SJZ-3	1.49	2.11	0.81	1.79
Central plain (II)	RQ-1	1.33	1.8	0.32	1.58
	HJ-1	1.34	1.84	0.56	1.54
	HJ-2	1.35	1.95	0.54	1.64
	WQ-1	1.33	1.95	0.44	1.54
	HS-1	1.42	1.75	0.16	1.57
Coastal plain (III)	CZ-1	1.37	1.77	0.21	1.57
	CZ-2	1.26	1.79	0.32	1.59
	HH-1	1.26	1.95	0.69	1.62
	QX-1	1.26	1.88	0.50	1.52
	QX-2	1.14	1.78	0.62	1.52

4. CONCLUSIONS

In this paper, ground temperature profiles and ground thermal conductivity for a piedmont alluvial plain, a central alluvial plain, and a coastal plain in the central NCP are investigated. Fifteen boreholes with depths of 100–150 m depth were drilled according to the local hydrogeological settings. Ground temperature profiles were measured through borehole logging. The thermo-physical parameters of drilling cores were measured in a laboratory. Moreover, double U-pipe BHEs were installed and CHTM-based TRTs were implemented to estimate the thermal properties in these boreholes.

Based on the vertical distribution of ground temperature in the three regions in central NCP, the profiles of ground temperature within 150 m in depth can be divided into three sections. The upper one, 10–15 m below the ground surface, is highly influenced by seasonal atmospheric conditions. The middle section, between 15 m and 40 m in depth, has a relatively constant ground temperature, and the deep section, below 40 m in depth, shows an obvious significant geothermal gradient ranging from 0.018 °C/m to 0.029 °C/m.

Thermal conductivity depends not only on particle size but also on groundwater flow. The laboratory measurements show that the thermal conductivity in the central NCP has an average thermal conductivity varying between 1.52 and 1.79 W/(m·K), with a standard deviation varying between 0.16 and 0.89. Thermal conductivity in the piedmont plain exhibits a larger variability than that of the central and coastal plain due to the significant heterogeneity of lithology. Based on the CHTM-based TRT method, the ground thermal conductivity is found to range between 2.37 and 2.68 W/(m·K) in the piedmont plain and varies between 1.35 and 1.94 W/(m·K) in the central and coastal plains. This finding shows that the piedmont plain has a higher potential for geothermal energy exploitation compared to the central and coastal plains.

Author Agreement: This study has been accepted and published by Energies.

REFERENCES

Badache, M., Eslami-Nejad, P., Ouzzane, M., Eslami-Nejad, P., Badache, M., Aidoun, Z., Lamarche, L.: A new modeling approach for improved ground temperature profile determination. *Renew. Energy* **2016**, *85*, 436–444.

Blum, P., Campillo, G., Münch, W., Kölbel, T.: CO_2 savings of ground source heat pump systems—A regional analysis. *Renew. Energy* **2010**, *35*, 122–127.

Cao, G., Han, D., Currell, M.J., Zheng, C.: Revised conceptualization of the North China Basin groundwater flow system: Groundwater age, heat and flow simulations. *J. Asian Earth Sci.* **2016**, *127*, 119–136.

Chen, W.H.: *Groundwater in Hebei*, Seismological Press: Beijing, China, 1999.

Foster, S., Garduno, H., Evans, R., Olson, D., Tian, Y., Zhang, W., Han, Z.: Quaternary Aquifer of the North China Plain—Assessing and achieving groundwater resource sustainability. *Hydrogeol. J.* **2004**, *12*, 81–93.

Kharazmi, A., Faraji, N., Hussin, R.M., Saion, E., Yunus, W.M., Behzad, K.: Structural, optical, opto-thermal and thermal properties of ZnS-PVA nanofluids synthesized through a radiolytic approach. *Beilstein. J. Nanotechnol.* **2015**, *6*, 529–536.

Li, X., Zhou, A., Gan, Y., Yu, T., Wang, D., Liu, Y.: Controls on the δ34S and δ18O of dissolved sulfate in the Quaternary aquifers of the North China Plain. *J. Hydrol.* **2011**, 400, 312–322.

Lunda, J.W., and Tothb, A.N.: Direct utilization of geothermal energy 2020 worldwide review. *Geothermics* **2021**, *90*, 101915.

Lu, X., Jin, M., van Genuchten, M.T., Wang, B.: Groundwater recharge at five representative sites in the Hebei Plain, China. *Ground Water* **2011**, *49*, 286–294.

Popiel, C.O., Wojtkowiak, J., Biernacka, B.: Measurement of temperature distribution in ground. *Exp. Therm. Fluid Sci.* **2001**, *25*, 301–309.

Shu, Y., Villholth, K.G., Jensen, K.H., Stisen, S., Lei, Y.: Integrated hydrological modeling of the North China Plain: Options for sustainable groundwater use in the alluvial plain of Mt. Taihang. *J. Hydrol.* **2012**, 464–465, 79–93.

Tao, S., Ru, M.Y., Du, W., Zhu, X., Zhong, Q.R., Li, B.G., Shen, G.F., Pan, X.L., Meng, W.J., Chen, Y.L.: Quantifying the rural residential energy transition in China from 1992 to 2012 through a representative national survey. *Nat. Energy* **2018**, *3*, 567–573.

van Manen, S.M., and Wallin, E.: Ground temperature profiles and thermal rock properties at Wairakei, New Zealand. *Renew. Energy* **2012**, *43*, 313–321.

Wang, H., Liu, B., Yang, F., Liu, F.: Test investigation of operation performance of novel split-type ground source heat pump systems for clean heating of rural households in North China. *Renew. Energy* **2021**, *163*, 188–197.

Wang, W., Wang, G., Zhu, X., Liu, Z.: Characteristics and potential of shallow geothermal resources in provincial capital cities of China. *Geology* **2017**, *44*, 1062–1073.

Wang, Y., Chen, Z., Duan, B., Shao, J.: Experimental evidence for hyperfiltration of saline water through compacted clay aquitard in the Hebei Plain. *J. Earth Sci.* **2014**, *25*, 1076–1082.

Xing, L., Guo, H., Zhan, Y.: Groundwater hydrochemical characteristics and processes along flow paths in the North China Plain. *J. Asian Earth Sci.* **2013**, 70–71, 250–264.

Xiong, Z., Fisher, D.E., Spitler, J.D.: Development and validation of a Slinky™ ground heat exchanger model. *Appl. Energy* **2015**, *141*, 57–69.

Zeng, H., Diao, N., Fang, Z.: Heat transfer analysis of boreholes in vertical ground heat exchangers. *Int. J. Heat Mass Transf.* **2003**, *46*, 4467–4481.

Zhang, Z.J., and Fei, Y.H.: *Atlas of Groundwater Sustainable Utilization in North China Plain*, Sinomaps Press: Beijing, China, 2009.

Zongyu, C., Jixiang, Q., Jianming, X., Jiaming, X., Hao, Y., Yunju, N.: Paleoclimatic interpretation of the past 30 ka from isotopic studies of the deep confined aquifer of the North China plain. *Appl. Geochem.* **2003**, *18*, 997–1009.